Quantifying Measurement Fluctuations from Stochastic Surface Processes on Sensors with Heterogeneous Sensitivity

Jérôme Charmet,[1] Thomas C. T. Michaels,[1] Ronan Daly,[2] Abhinav Prasad,[3] Pradyumna Thiruvenkathanathan,[3] Robin S. Langley,[4] Tuomas P. J. Knowles,[1] and Ashwin A. Seshia[3]

[1]*Department of Chemistry, University of Cambridge, Lensfield Road, Cambridge, CB2 1EW, United Kingdom*

[2]*Institute for Manufacturing, Department of Engineering, University of Cambridge, Charles Babbage Road, Cambridge, CB3 0FS, United Kingdom*

[3]*Nanoscience Centre, Department of Engineering, University of Cambridge, 11 J. J. Thomson Avenue, Cambridge, CB3 0FF, United Kingdom*

[4]*Department of Engineering, University of Cambridge, Trumpington Street, Cambridge, CB2 1PZ, United Kingdom*

(Received 19 March 2016; revised manuscript received 22 April 2016; published 27 June 2016)

Recent advances in micro- and nanotechnology have enabled the development of ultrasensitive sensors capable of detecting small numbers of species. In general, however, the response induced by the random adsorption of a small number of objects onto the surface of such sensors results in significant fluctuations due to the heterogeneous sensitivity inherent to many such sensors coupled to statistical fluctuations in the particle number. At present, this issue is addressed by considering either the limit of very large numbers of analytes, where fluctuations vanish, or the converse limit, where the sensor response is governed by individual analytes. Many cases of practical interest, however, fall between these two limits and remain challenging to analyze. Here, we address this limitation by deriving a general theoretical framework for quantifying measurement variations on mechanical resonators resulting from statistical-number fluctuations of analyte species. Our results provide insights into the stochastic processes in the sensing environment and offer opportunities to improve the performance of mechanical-resonator-based sensors. This metric can be used, among others, to aid in the design of robust sensor platforms to reach ultrahigh-resolution measurements using an array of sensors. These concepts, illustrated here in the context of biosensing, are general and can therefore be adapted and extended to other sensors with heterogeneous sensitivity.

DOI: 10.1103/PhysRevApplied.5.064016

I. INTRODUCTION

Micro- and nanotechnologies have experienced dramatic development in the past decades leading to the fabrication of sensors capable of reaching the high sensitivities and resolutions required for the detection of small numbers [1–5] or single molecules [6]. Such developments have resulted in many applications ranging from the early diagnosis of diseases [7,8] to food safety [9]. While measurements of a large number of objects are accurately described by the average response of the sensor, the significant measurement variations associated with the adsorption of far smaller numbers of molecules onto the surface of the sensor have represented a limitation in the practical applicability of high-resolution sensing. Such measurement variations arise from the heterogeneous sensitivity across the surface of many nano- and microfabricated sensors as well as from the statistical variation in the number and mass of the species bound to the sensor. For instance, in mechanical resonators—where the response function arises from the spatial variation of their vibrational mode shapes—the same number of objects of identical mass can induce different responses depending on their location on the sensor surface. Figure 1(b) shows the frequency shifts induced by four identical polystyrene particles of 10-μm diameter positioned at different locations [Fig. 1(a)] on a micromechanical resonator excited in the Lamé mode (see Supplemental Material [10] for details). In this case, a measurement variation of approximately 30% is observed between measurements i and iii [Fig. 1(b)]. This fundamental issue has also been identified for localized plasmon sensing [11] and impedance measurements [12] as well as for field-effect transistors, where a sensitivity dependence based on the number of molecules [13] as well as their position [14] is reported. This problem is particularly relevant to nanofabricated sensors, as the dimensions of such sensors are comparable to the size of the objects to be detected. Thus, in order to exploit the full potential offered by micro- and nanofabricated sensors for detecting small numbers of analytes, it is of fundamental importance to understand and quantify the nature of stochastic processes in the sensing environment.

At present, the issue of heterogeneous sensitivity is usually dealt with by considering two operational regimes

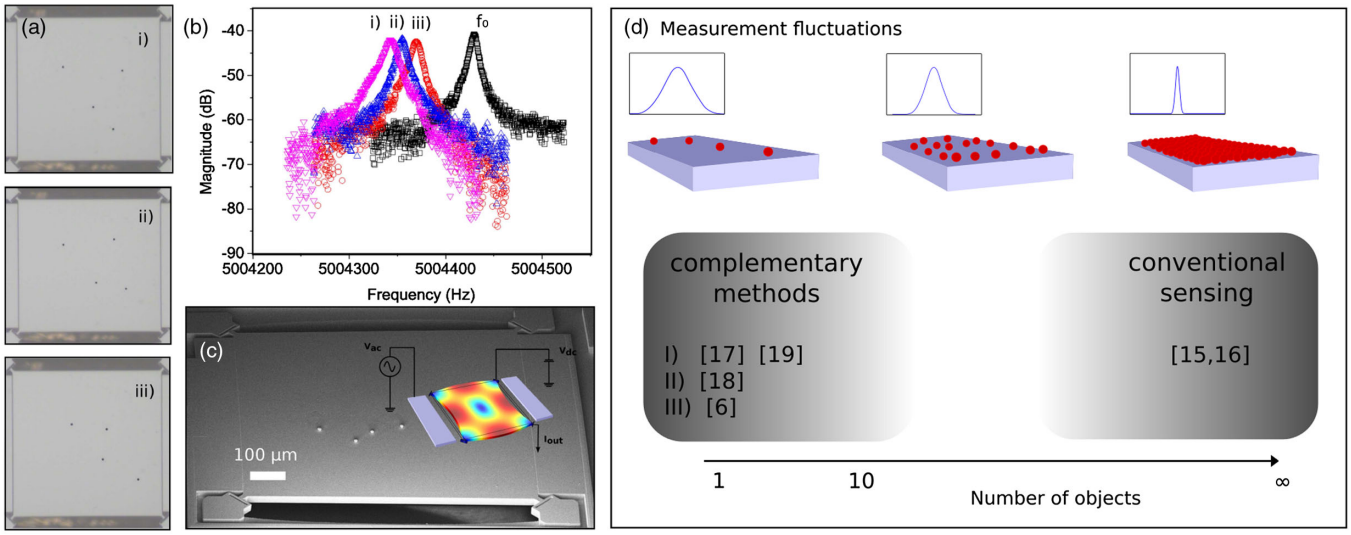

FIG. 1. Effect of the position-dependent sensitivity of mechanical resonators operating as gravimetric sensors and regimes of operation. (a) Images of four polystyrene (PS) particles of 10-μm diameter on a square plate resonator excited in the Lamé mode for three cases studied. (b) The amplitude response at resonance for each of the three cases presented and f_0, the resonant frequency without mass loading. (c) Scanning electron micrograph showing four PS particles on a square plate resonator and the measurement principle (inset). (d) When the number of objects is large, the average response resolves the measurement accurately. This assumption is valid for the case of distributed mass using thin-film deposition, for example (see Refs. [15,16]). When the number of objects is small, the fluctuations become very large and complementary methods are necessary to resolve the measurements. Multimodal approaches (I) are used to measure single objects [17] and up to three beads in Ref. [18]. Transfer-function methods (II) and physicochemical methods (III) are used to detect single objects [19] and [6], respectively. However, the interpretation of results falling between these two regimes, that represent many cases of practical interest, are not described by current models.

that depend on the number of objects located on the surface of the sensor [see Fig. 1(d)]. In the first regime, when the number of objects to be detected is very large, or in the case of uniformly distributed mass [15,16], the measurement is accurately resolved by using the averaged sensor response. However, due to the lack of a generally applicable metric, it was unclear until now how many objects are needed to operate in this regime without introducing large measurement variations. In the second regime, if only a small number of objects are randomly positioned on the sensor, complementary methods have been developed to describe the measured response. In the case of mechanical resonators, these alternative methods include multimodal approaches, which have enabled the detection of single proteins [20] and microparticles [17], transfer-function methods, used to detect single microbeads [19], and physicochemical methods that precisely position the objects on areas of high sensitivity and have enabled the detection of single DNA molecules [6]. However, while these methods are well suited for the detection of one or a few objects, they are not easily scalable to tens of objects. For example, the use of multimodal approaches is limited by the number of modes studied [5,18], which currently sets a practical transduction limit for this approach. Notable exceptions include sensors operating in the flow-through regime [3] and sensors that rely on real-time sensing strategies [20]. However, in both cases, the small dimensions of these types of sensors, necessary to meet the sensitivity conditions to detect small amounts of molecules, can seriously limit their performance. In the case of sensors operating in the flow-through regime, the size of the channels restricts the volume that can be probed over a reasonable time (see, for example, Ref. [3]). In the case of real-time sensing, even though nanomechanical resonators have been used in the gas phase [20], their operation in liquid media for affinity-based sensing, for example, is limited by the small area available to bind the analytes of interest [21].

Despite these recent developments, many cases of practical interest, including the early detection of diseases as illustrated later, fall in between the two regimes mentioned above [Fig. 1(d)]. In this paper, we address this limitation by deriving a general theoretical framework that describes the measurement variations induced by any number of objects randomly positioned on a sensor with heterogeneous sensitivity. This metric can be used to define the limit between the above regimes of operation and, importantly, offers opportunities to design robust sensor platforms to reach ultrahigh-resolution measurements, as we illustrate in the context of biosensing using an array of microresonators. In addition, our metric provides further insights into stochastic processes in the sensing environment, a problem which has recently been identified as one of the major challenges in micro- and nanomechanical

biosensing [22]. Without loss of generality, the results are presented for mechanical resonators. This sensor platform is chosen because the response of such sensors depends on the spatial variations of their mode shape, and, therefore, the findings in this study apply to mechanical resonators of all length scales. In fact, our general framework can be extended to other sensors with heterogeneous sensitivity. We anticipate, therefore, that our results will have a positive impact on many micro- and nanofabricated sensors and will find a particular relevance in the field of biosensing where an early diagnosis relies on the measurement of a small quantity of biomolecules [2–4,7,8].

II. MEASUREMENT VARIATIONS

A. General expression

In order to evaluate the measurement variations induced by a random number of objects N with variable mass m_j randomly positioned on a gravimetric sensor operating in the dynamic mode, we study the relative variance of the total added effective mass $\Delta\tilde{m}$ reported by the sensor upon exposure to added masses m_j (see Ref. [23]):

$$\Delta\tilde{m} = \sum_{j=1}^{N} m_j |\varphi(\boldsymbol{x}_j)|^2, \tag{1}$$

where $\varphi(\boldsymbol{x})$ is the mode shape scaled to the unit-generalized mass such that $1/A\int|\varphi(\boldsymbol{x})|^2 d\boldsymbol{x} = 1/M$, with A being the sensor surface area and M its effective mass. The relative variance is given by $\sigma^2/\mu^2 = \mathrm{Var}[\Delta\tilde{m}]/\mathbb{E}[(\Delta\tilde{m})]^2$, where $\mathrm{Var}[\Delta\tilde{m}] = \mathbb{E}[(\Delta\tilde{m})^2] - \mathbb{E}[(\Delta\tilde{m})]^2$ and the expectation values are averages over the sensor surface, as well as the number and mass of the placed objects. The expectation value of the total added effective mass can be computed as

$$\mathbb{E}[\Delta\tilde{m}] = \frac{\langle N\rangle\langle m\rangle}{M}. \tag{2}$$

From Eq. (1), we can calculate

$$\begin{aligned}(\Delta\tilde{m})^2 &= \sum_{i=1}^{N}\sum_{j=1}^{N} m_i m_j \varphi^2(\boldsymbol{x}_i)\varphi^2(\boldsymbol{x}_j) \\ &= \sum_{i=1}^{N} m_i^2 \varphi^4(\boldsymbol{x}_i) + \sum_{i=1}^{N}\sum_{j\neq i} m_i m_j \varphi^2(\boldsymbol{x}_i)\varphi^2(\boldsymbol{x}_j)\end{aligned} \tag{3}$$

and hence

$$\mathbb{E}[(\Delta\tilde{m})^2] = \langle N\rangle\langle m^2\rangle\mathbb{E}[\varphi^4(\boldsymbol{x}_i)] + \frac{\langle N(N-1)\rangle\langle m\rangle^2}{M^2}. \tag{4}$$

Combining Eq. (2) with Eq. (4) and using $\langle m^2\rangle = \sigma_m^2 + \mu_m^2$, we obtain the relative variance

$$\frac{\sigma^2}{\mu^2} = \frac{1}{\mu_n}\left\{M^2\left(1+\frac{\sigma_m^2}{\mu_m^2}\right)\mathbb{E}[\varphi^4(\boldsymbol{x}_j)] - 1\right\} + \frac{\sigma_n^2}{\mu_n^2}, \tag{5}$$

where $\mu_{m,n}$ and $\sigma_{m,n}$ are the averages and standard deviations of the mass and number distribution of the loaded objects, respectively, and $\mathbb{E}[|\varphi(\boldsymbol{x})|^4] = 1/A\int|\varphi(\boldsymbol{x})|^4 d\boldsymbol{x}$. The detailed derivation can be found in Supplemental Material [10]. Equation (5) establishes a general framework for the quantification of measurement fluctuations due to stochastic processes in the sensing environment. The limiting case of a sensor with homogeneous sensitivity can be derived from Eq. (5) and is given by $\sigma^2/\mu^2 = (\sigma_m^2/\mu_m^2)/\mu_n + \sigma_n^2/\mu_n^2$.

Figure 2(a) shows the relative variance of measurements in the case of a square plate resonator excited in the Lamé mode and loaded with objects of variable mass distribution, as described by increasing coefficients of variation ($c_v = \sigma_m/\mu_m$). The relative variance increases, as expected, with the coefficient of variation.

B. Special case: Fixed number of objects N and mass m

A case of practical interest is the situation when a given number of objects N of identical mass is measured, corresponding to $\sigma_m = 0$ and $\sigma_n = 0$ in Eq. (5):

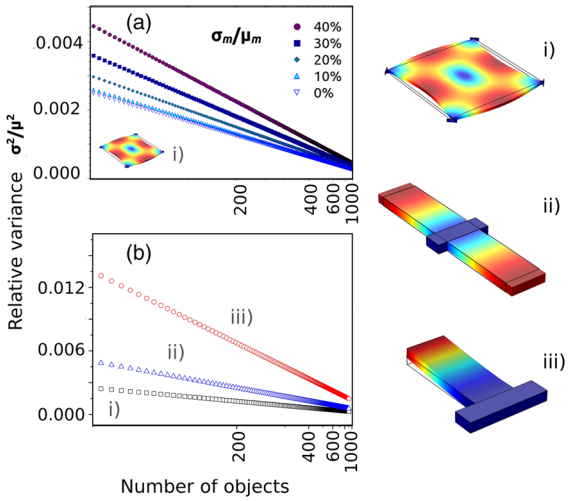

FIG. 2. Relative variance as a function of the number of objects on the sensor [see Eq. (5)]. (a) The effect of stochastic processes in the sensing environment. A graph showing the relative variance as a function of the inverse of the number of objects for a square resonator excited in the Lamé mode. The relative variance increases with the coefficient of variation ($c_v = \sigma_m/\mu_m$), which represents the ratio of the width of the mass distribution to the mean. (b) The case of a given number of objects of identical mass ($\sigma_m = 0$ and $\sigma_n = 0$). Three sensors are compared: a square plate resonator excited in the Lamé mode (i), a beam excited in its first extensional mode (ii), and a cantilever excited in its first flexural mode (iii). The mode shapes of each resonator (top to bottom) are presented on the right.

$$\frac{\sigma^2}{\mu^2} = \frac{1}{N}\{M^2\mathbb{E}[|\varphi(\boldsymbol{x})|^4] - 1\}. \quad (6)$$

Because $\mathbb{E}[|\varphi(\boldsymbol{x})|^4] \propto M^{-2}$, it can be seen that Eq. (6) depends solely on the number of loaded objects and the mode shape of the sensor studied. This observation suggests that the resulting metric σ^2/μ^2 can be used to compare the performance of different types of resonators. Figure 2(b) shows the relative variance [Eq. (6)] plotted against the inverse of the number of objects for three common gravimetric micro- or nanomechanical sensors: a square plate resonator excited in the Lamé mode, a beam excited in its first extensional mode, and a beam (cantilever) excited in its first flexural mode. The figure shows that the relative variance decreases linearly with the inverse number of objects at a rate that depends on the mode shape of the sensor. It is observed also that a square plate resonator excited in the Lamé mode presents lower measurement variations compared to the other resonators mentioned above. This advantage becomes less pronounced as the number of objects increases, $N \to \infty$, as in this case variations become negligible for all resonator types. This situation represents the first regime of operation mentioned earlier.

C. Metrics and limits of detection

One of the most widely used metrics to quantify the performance of gravimetric sensors is their gravimetric limit of detection. In this section, we show that the expression can serve as a complementary metric to define a numeral limit of detection or, in other words, the minimum number of objects necessary to obtain a measurement of a given precision.

Let us consider the case of the square resonator described in the introduction [Fig. 1(c)]. Taking into account the electronics and equipment noise, that can be extracted from the frequency-noise floor, the gravimetric limit of detection of the sensor is defined by $\Delta f = (d\phi/df)^{-1}\Delta\phi$, where $(d\phi/df)$ is the slope of the phase at resonance frequency and the phase noise $\Delta\phi$ is taken as the standard deviation of the zero-span phase-noise data (see Fig. S2). In our case, the short-term frequency-noise floor is 9×10^{-4} Hz, yielding a gravimetric limit of detection of approximately 2 fg, which is much lower than individual PS particles (approximately 0.52 ng) used experimentally. Using Eq. (6), one can calculate that 100 objects, which corresponds to 52 ng for PS particles of 10-μm diameter, are necessary to obtain measurements with a relative standard deviation of 5%.

This observation should be put in perspective with the fact that the gravimetric limit of detection of 1 ag, which corresponds to 25 molecules of approximately 24 kDa, has been reached by a variety of biosensors [3,4,24]. This number of molecules, that falls between the two regimes of operation described above, shows the importance of tackling the issue of the heterogeneous sensitivity in parallel with the development of more sensitive sensors. We show in the following section how the metrics derived in this paper can be used to address this issue.

III. APPLICATION TO BIOSENSING

A. Design rules for sensing platform

In this section, we show that Eq. (6) enables the establishment of design rules to develop sensor platforms, comprised of arrays of sensors, capable of reaching ultrahigh resolutions. This solution, particularly appropriate for micro- or nanomechanical sensors that are conventionally fabricated in arrays, is made possible by using a simple statistical concept. In addition, unlike the complementary methods conventionally associated with high-resolution measurements, the method proposed here enables the measurement of any number of objects.

Within this framework, we can estimate the mean value of the number of analytes, within a given precision, provided that the standard deviation of the population is known for a given sample size. This approach is described by the maximum error of the estimate, given by $E = z_{\alpha/2}\sigma/\sqrt{n}$, where $z_{\alpha/2}$ is the standard score, σ the standard deviation, and n the sample size. In the case where the standard deviation of the population is unknown, however, it is necessary to obtain a large sample size to accurately estimate the mean as illustrated by Fig. 3, that shows the normalized normal distribution obtained using a Monte Carlo simulation (detailed later) for different numbers of objects. The insets show the distributions corresponding to 200 objects for sample sizes of 2000 and 200 measurements, (i) and (ii), respectively. In our case, the standard deviation can be calculated using Eq. (6). Defining

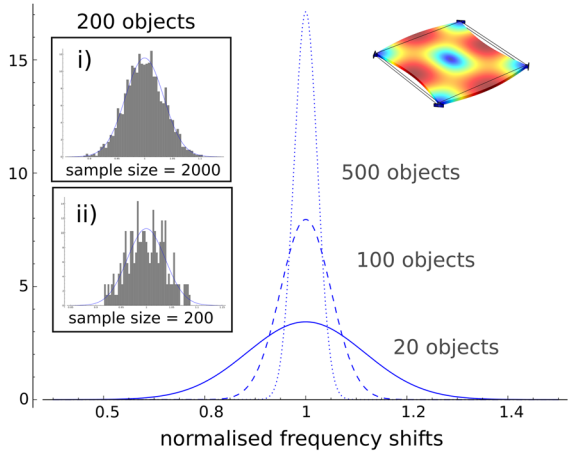

FIG. 3. Results from Monte Carlo simulations for a square resonator excited in the Lamé mode. The normal distributions represent the normalized frequency shift for 20, 100, and 500 objects and a sample size of 2000. The inset (left) shows the normal distribution associated with 200 objects for a sample size of 200 (i) and 2000 measurements (ii). The inset (right) shows the mode shape of the resonator.

the maximum acceptable standard deviation of $\sigma_{\max}$ for a given application, the maximum error for one measurement ($n = 1$) is $E_1 = z_{\alpha/2}\sigma_{\max}$. Therefore, the minimum number of independent measurements $n_{\min}$ necessary to reach the same error E_1 for a population of given standard deviation σ_i becomes

$$n_{\min} = \frac{\sigma_i^2}{\sigma_{\max}^2}. \tag{7}$$

In other words, if a sensor yields measurements with large (known) standard deviations σ_i, it is possible to reach a higher level of precision (defined here by the maximum-permitted standard deviation $\sigma_{\max}$) by repeating the measurements a certain number of times $n_{\min}$. It should be noted that the application of this simple concept is possible only with an *a priori* knowledge of the measurement variation, which is now provided by Eq. (6). In the case of biosensing, where the measurements are stochastic in nature, an array of sensors generates independent measurements that can be used to decrease the limit of detection according to the concept described above.

The application of this principle is illustrated below using a practical example for the detection of protein-specific antigen (PSA), a biomarker for prostate cancer, given a set of realistic constraints. We show how the quantification of the measurement variations, enabled by our theoretical platform, can contribute to the design of robust, highly sensitive sensor platforms capable of high-resolution measurements. Assuming that an ideal sensor should be able to detect small mass variations on a daily basis, for example, to monitor the efficiency of a treatment, we require that 95% of the measurements fall within 5% of the mean (2σ rule). For a square resonator excited in the Lamé mode, a beam excited in the extensional mode, and a cantilever excited in its first flexural mode, we find that the minimum number $N_{\min}$ of objects necessary to reach this condition, as calculated using Eq. (6), is $N_{\min} = 1600$, $N_{\min} = 3200$, and $N_{\min} = 8500$, respectively. Among the sensors compared, the square plate resonator excited in the Lamé mode represents the best option. That is, it requires fewer objects to reach the same precision. The clinical limit of the detection of PSA is 0.1 ng ml^{-1} [7].

Assuming that the transport of the molecules to the biosensor has been optimized, i.e., the sensor operates in a reaction-limited regime, one can use the Langmuir isotherm to calculate the surface concentration of receptors (capture molecules) bound by target molecules at equilibrium. This assumption is valid for the sensors studied here over a wide range of dimensions and conditions, as detailed in Supplemental Material [10]. If we assume that the gravimetric limit of detection and the desired sensitivity (both functions of the dimensions of the sensor; see, for example, Ref. [25]) limit the lateral dimension of the sensor to 10 μm at most, we find that a maximum of 134 molecules of PSA are bound at equilibrium using IgG capture molecules with an average binding density $b_m = 6.5 \times 10^{11}$ cm^{-2} [26] and association and dissociation constants $K_{\text{on}} = 2.2 \times 10^4$ M^{-1} s^{-1} and $K_{\text{off}} = 3.2 \times 10^{-4}$ s^{-1} [27], respectively. This number of molecules is below the 1600 molecules required to reach the precision conditions defined above. Calculating the relative variance induced by $N = 134$ molecules on a square resonator excited in the Lamé mode using Eq. (6) and combining the result with Eq. (7), we find that 12 independent measurements are sufficient to estimate the mean of the measurement within the defined precision condition. Therefore, an array of 12 square resonators of 10-μm side length enables the detection of PSA down to 0.1 ng ml^{-1} for the precision, resolution, and sensitivity constraints defined above.

We note that in practical cases it is unlikely that an exact number $N = 134$ of molecules will bind to the surface of the sensor. In order to take this situation into consideration, we come back to the general expression [Eq. (5)] and consider the case where $\sigma_N/\mu_N = 2.5\%$ (i.e., the number of molecules varies between 127 and 141 in 95% of the cases on each sensor). We find that an array of 16 resonators is necessary to reach the same resolution.

B. Other practical cases

Let us now consider the more complicated situation where a given number of objects N of variable mass distribution are loaded on the sensor. Figure 2(b) shows that the relative variance increases with the coefficient of variation. This result has direct practical implications to at least two important biological processes. First, in the case of the measurement of biomolecules in a liquid and sensed using a mechanical resonator, the frequency shifts recorded are induced by their solvated mass rather than their dry mass; i.e., the response depends on the mass of the molecules and that of the solvent they drag. However, the amount of solvent dragged by the molecule of interest depends on their packing on the surface of the sensor [28]. In this case, Eq. (5) can be used to take these variations into consideration by adapting the coefficient of variations. Second, the same equation can be used to study the biological noise reported for many biosensors based on mechanical resonators [6,29,30]. Affinity-based biosensors rely on capture molecules such as antibodies attached to the surface of the sensor to capture the biomolecule of interest. However, even though appropriate passivation layers can prevent strong and lasting interaction between unwanted molecules and the sensors, transient interactions cannot be completely eliminated. Such interactions result in a background measurement noise due to the spatial sensitivity of the sensor. One can use Eq. (5) to assess the effect of a number of unwanted molecules (of different masses) on the sensor. Assuming a number of unwanted molecules N whose masses are distributed with a fixed coefficient of

variation c_v, Fig. 2(a) shows the relative variance expected for different cases.

C. Monte Carlo simulation

An independent Monte Carlo model is developed for the purpose of the study to verify the validity of Eq. (6) and to give further insights into stochastic processes on resonators. The model is based on Eq. (1) and calculates the total added effective mass for a given number of objects N positioned at randomly generated coordinates. The model assumes no interaction between the objects and represents measurements in the linear regime where the principle of superposition can be applied. These assumptions are valid in the cases studied in this paper, as we are considering only a small number of lightweight objects. The model also assumes a purely gravimetric interaction between the object and the resonator's surface. Statistical data, normalized to simplify comparisons, extracted from a population of 5000 measurement agree within 3% with Eq. (6). For 2000 measurements the variations can go up to 4%, while for 500 measurements they can reach up to 8%. Figure 3 shows the normalized normal simulation for different numbers of objects. The insets show the distributions corresponding to 200 objects for sample sizes of 2000 and 200 measurements, (i) and (ii), respectively. Further details can be found in Supplemental Material [10].

In this section, we examine how an adapted version of the Monte Carlo simulations gives further insights into nonspecific interactions on a cantilever excited in its first flexural mode. In this case, the model is adapted to produce a series of discrete measurements, where each measurement is reported as a function of an arbitrary time unit, instead of being averaged for a given measurement population. Such a model is used here to show measurement variations as a function of time. Consider a hypothetical experiment where the measurement sampling time τ_n is shorter than the interaction between the unwanted molecules and the sensor, such that, every time a measurement is taken, the same number of unwanted molecules of mass m_u interact with the resonator. This case is captured by Fig. 4, that shows the measurement variations induced by 50 and 500 molecules, respectively. It can be seen that the figure appears like a noisy measurement, suggesting that nonspecific interaction with unwanted molecules can contribute to the biological noise observed on many biosensors based on mechanical resonators [6,29,30]. It should be noted, however, that, even though the discrete Monte Carlo model provides a visual clue to the type of measurement variations that can be expected due to nonspecific interaction, the general framework presented [Eq. (5)] that accounts for the number and mass variation gives more insights into this complex subject. However, this study falls outside the scope of this paper and will be addressed in future research.

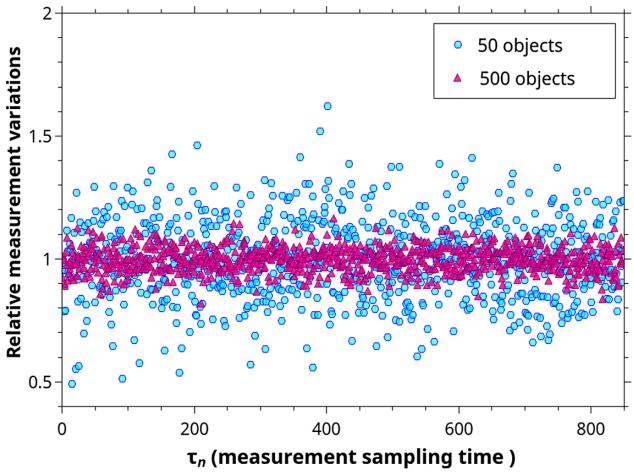

FIG. 4. Results from a discretized version of the Monte Carlo simulations model showing that nonspecific interaction (transient binding and dissociation events) on a sensor with heterogeneous gravimetric sensitivity, in this case a cantilever excited in its first flexural mode, can appear as a noisy measurement (the variations decrease with the number of objects).

IV. CONCLUSIONS

Finally, we note that our results, which are discussed in the context of mechanical sensors operating in the dynamic mode, are general and can be extended to other types of sensors when the measured output O_s in response to a variation in the input quantity y obeys the relationship $O_s = \sum_{j=1}^{N} y_j \phi(\boldsymbol{x}_j)$, where $\phi(\boldsymbol{x}_j)$ represents the location-dependent sensitivity map. In the case studied in the paper, $O_s = \Delta\tilde{m}$ [23], $y_j = m_j$, and $\phi(\boldsymbol{x}_j) = |\varphi(\boldsymbol{x}_j)|^2$, where $\varphi(\boldsymbol{x}_j)$ is the mode shape scaled to the unit generalized mass.

In conclusion, we have developed a general framework to study stochastic processes on the surface of mechanical sensors operating in the dynamic mode. We have quantified the measurement variations induced by a variable number of objects of varying mass randomly positioned on the sensor. This metric can be used to compare the performance of any gravimetric sensor based on mechanical resonators, and importantly it enables the design of sensor platforms with improved performance. Using an array of sensors, a solution particularly relevant to micro- and nanosensors, it is possible to reach an ultrahigh-resolution measurement of any number of objects. This solution does not require the implementation of the complementary methods normally associated with this regime of operation and enables the measurement of the small quantities of molecules or cells relevant to the early detection of diseases. In addition, our theoretical framework can be used to study other stochastic processes in the sensing environment. It can also give insight into biological noise due to nonspecific interaction, and it could also be adapted to study the motility of cells or the effect of cooperative binding, for example. Finally, since our framework can be adapted to other sensor

platforms, we anticipate, due in particular to great interest in high-resolution sensing, that the metric developed in the present paper will be relevant to researchers developing or working with sensors across a variety of fields.

ACKNOWLEDGMENTS

We acknowledge funding from the W. D. Armstrong fund, Biotechnology and Biological Sciences Research Council, Newman Foundation, St. John's College–University of Cambridge, and European Research Council.

J. C. and T. C. T. M. contributed equally to this work.

[1] G. Shalev, G. Landman, I. Amit, Y. Rosenwaks, and I. Levy, Specific and label-free femtomolar biomarker detection with an electrostatically formed nanowire biosensor, NPG Asia Mater. **5**, e41 (2013).

[2] J. M. Nam, C. S. Thaxton, and C. A. Mirkin, Nanoparticle-based bio-bar codes for the ultrasensitive detection of proteins, Science **301**, 1884 (2003).

[3] S. Olcum *et al.*, Weighing nanoparticles in solution at the attogram scale, Proc. Natl. Acad. Sci. U.S.A. **111**, 1310 (2014).

[4] R. de la Rica and M. M. Stevens, Plasmonic ELISA for the ultrasensitive detection of disease biomarkers with the naked eye, Nat. Nanotechnol. **7**, 821 (2012).

[5] M. S. Hanay, S. I. Kelber, C. D. O'Connell, P. Mulvaney, J. E. Sader, and M. L. Roukes, Inertial imaging with nanomechanical systems, Nat. Nanotechnol. **10**, 339 (2015).

[6] B. Ilic, Y. Yang, K. Aubin, and R. Reichenbach, Enumeration of DNA molecules bound to a nanomechanical oscillator, Nano Lett. **5**, 925 (2005).

[7] D. Giljohann and C. Mirkin, Drivers of biodiagnostic development, Nature (London) **462**, 461 (2009).

[8] D. M. Rissin *et al.*, Single-molecule enzyme-linked immunosorbent assay detects serum proteins at subfemtomolar concentrations, Nat. Biotechnol. **28**, 595 (2010).

[9] C. A. Batt, Food pathogen detection, Science **316**, 1579 (2007).

[10] See Supplemental Material at http://link.aps.org/supplemental/10.1103/PhysRevApplied.5.064016 for additional information about (i) the experimental details, (ii) the derivation of the relative variance, (iii) the transport and reaction of analytes, and (iv) the Monte Carlo simulation.

[11] O. Kedem, A. Vaskevich, and I. Rubinstein, Critical issues in localized plasmon sensing, J. Phys. Chem. C **118**, 8227 (2014).

[12] S. Grimnes and O. G. Martinsen, Sources of error in tetrapolar impedance measurements on biomaterials and other ionic conductors, J. Phys. D **40**, 9 (2007).

[13] F.-S. Zhou and Q.-H. Wei, Scaling laws for nanoFET sensors, Nanotechnology **19**, 015504 (2008).

[14] M. W. Shinwari, M. J. Deen, and P. R. Selvaganapathy, Finite-element modelling of biotransistors, Nanoscale Res. Lett. **5**, 494 (2010).

[15] A. Cagliani and Z. J. Davis, Ultrasensitive bulk disk microresonator-based sensor for distributed mass sensing, J. Micromech. Microeng. **21**, 045016 (2011).

[16] A. Prasad, J. Charmet, and A. A. Seshia, Simultaneous interrogation of high-Q modes in a piezoelectric-on-silicon micromechanical resonator, Sens. Actuators A **238**, 207 (2016).

[17] S. Dohn, W. Svendsen, A. Boisen, and O. Hansen, Mass and position determination of attached particles on cantilever based mass sensors, Rev. Sci. Instrum. **78**, 103303 (2007).

[18] S. Dohn, S. Schmid, F. Amiot, and A. Boisen, Position and mass determination of multiple particles using cantilever based mass sensors, Appl. Phys. Lett. **97**, 044103 (2010).

[19] D. Kim, S. Hong, J. Jang, and J. Park, Simultaneous determination of position and mass in the cantilever sensor using transfer function method, Appl. Phys. Lett. **103**, 033108 (2013).

[20] M. S. Hanay, S. Kelber, A. K. Naik, D. Chi, S. Hentz, E. C. Bullard, E. Colinet, L. Duraffourg, and M. L. Roukes, Single-protein nanomechanical mass spectrometry in real time, Nat. Nanotechnol. **7**, 602 (2012).

[21] T. M. Squires, R. J. Messinger, and S. R. Manalis, Making it stick: Convection, reaction and diffusion in surface-based biosensors, Nat. Biotechnol. **26**, 417 (2008).

[22] J. L. Arlett, E. B. Myers, and M. L. Roukes, Comparative advantages of mechanical biosensors, Nat. Nanotechnol. **6**, 203 (2011).

[23] It is noted that, in practice, the quantity measured to account for a mass change on a mechanical resonator is its resonance frequency. The frequency shift Δf associated with the addition of a mass load Δm (ignoring stiffness changes) can be approximated to the first order by $\Delta f = -(1/2)(\Delta m/m_{\mathrm{eff}})f_o$, where m_{eff} is the effective mass of the resonator and f_o its resonance frequency.

[24] B. Ilic *et al.*, Attogram detection using nanoelectromechanical oscillators, J. Appl. Phys. **95**, 3694 (2004).

[25] E. Gil-Santos, C. Baker, D. T. Nguyen, W. Hease, C. Gomez, A. Lemaître, S. Ducci, G. Leo, and I. Favero, High-frequency nano-optomechanical disk resonators in liquids, Nat. Nanotechnol. **10**, 810 (2015).

[26] S. Zhang, A. Garcia-D'Angeli, J. P. Brennan, and Q. Huo, Predicting detection limits of enzyme-linked immunosorbent assay (ELISA) and bioanalytical techniques in general, Analyst **139**, 439 (2014).

[27] F. Yu, B. Persson, S. Lofas, and W. Knoll, Surface plasmon fluorescence immunoassay of free prostate-specific antigen in human plasma at the femtomolar level, Anal. Chem. **76**, 6765 (2004).

[28] K. Xu, M. M. Ouberai, and M. E. Welland, A comprehensive study of lysozyme adsorption using dual polarization interferometry and quartz crystal microbalance with dissipation, Biomaterials **34**, 1461 (2013).

[29] M. Calleja, P. M. Kosaka, A. San Paulo, and J. Tamayo, Challenges for nanomechanical sensors in biological detection, Nanoscale **4**, 4925 (2012).

[30] M. G. Von Muhlen, N. D. Brault, S. M. Knudsen, S. Jiang, and S. R. Manalis, Label-free biomarker sensing in undiluted serum with suspended microchannel Resonators, Anal. Chem. **82**, 1905 (2010).